

# PL-embedding the dual of $J^2$ -gems into $\mathbb{S}^3$ by an $O(n^2)$ -algorithm \*

Sóstenes Lins and Ricardo Machado

May 28, 2013

## Abstract

Let be given a *colored 3-pseudo-triangulation*  $\mathcal{H}^*$  with  $n$  tetrahedra. Colored means that each tetrahedron have vertices distinctively colored 0,1,2,3. In a *pseudo* 3-triangulation the intersection of simplices might be subsets of simplices of smaller dimensions, instead of singletons of such faces, as for true triangulations. If  $\mathcal{H}^*$  is the dual of a  $J^2$ -gem (shortly defined), then we show that  $|\mathcal{H}^*|$  is  $\mathbb{S}^3$  and we make available an  $O(n^2)$ -algorithm to produce a PL-embedding ([10]) of  $\mathcal{H}^*$  into  $\mathbb{S}^3$ . This is rather surprising because such PL-embeddings are often of exponential size. This work is the first step towards obtaining, via an  $O(n^2)$ -algorithm, a framed link presentation inducing the same closed orientable 3-manifold as the one given by a colored pseudo-triangulation. Previous work on this topic appear in [5], [6] and [7]. However, the exposition and the new proofs of this paper are meant to be entirely self-contained.

## 1 Introduction

### 1.1 $J^2$ -gems

A  $J^2$ -gem is a 4-regular, 4-edge-colored planar graph  $\mathcal{H}$  obtained from the intersection pattern of two Jordan curves  $X$  and  $Y$  with  $2n$  transversal crossings. These crossings define consecutive segments of  $X$  alternatively inside  $Y$  and outside  $Y$ . Color the first type 2 and the second type 3. The crossings also define consecutive segments of  $Y$  alternatively inside  $X$  and outside  $X$ . Color the first type 0 and the second type 1. This defines a 4-regular 4-edge-colored graph  $\mathcal{H}$  where the vertices are the crossings and the edges are the colored colored segments. Let  $\mathcal{H}^*$  be the 3-dimensional abstract 3-complex formed by taking a set of vertex colored tetrahedra in 1–1 correspondence with the set of vertices of  $\mathcal{H}$ ,  $V(\mathcal{H})$ , so that each tetrahedra has vertices of colors 0,1,2,3. This vertex coloring induces a face coloring of the triangular faces of the tetrahedron: color  $i$  the face opposite to the vertex colored  $i$ . For each  $i$ -colored edge of  $\mathcal{H}$  with ends  $u$  and  $v$  paste the corresponding tetrahedra  $\nabla_u$  and  $\nabla_v$  so as to paste the two triangular faces that do not contain a vertex of color  $i$  in such a way as to match vertices of the other three colors. We show that the topological space  $|K|$  induced by  $\mathcal{H}^*$  is  $\mathbb{S}^3$ . Moreover we describe an  $O(n^2)$ -algorithm to make available a PL-embedding ([10]) of  $\mathcal{H}^*$  into  $\mathbb{S}^3$ . We get explicit coordinates in  $\mathbb{S}^3$  for the 0-simplices and the  $p$ -simplices ( $p \in \{1, 2, 3\}$ ) are linear simplices in the spherical geometry.

---

\*2010 Mathematics Subject Classification: 57M25 and 57Q15 (primary), 57M27 and 57M15 (secondary)

## 1.2 Gems and their duals

A  $(3+1)$ -graph  $\mathcal{H}$  is a connected regular graph of degree 4 where to each vertex there are four incident differently colored edges in the color set  $\{0, 1, 2, 3\}$ . For  $I \subseteq \{0, 1, 2, 3\}$ , an  $I$ -residue is a component of the subgraph induced by the  $I$ -colored edges. Denote by  $v(\mathcal{H})$  the number of 0-residues (vertices) of  $\mathcal{H}$ . For  $0 \leq i < j \leq 3$ , an  $\{i, j\}$ -residue is also called an  $ij$ -gon or an  $i$ - and  $j$ -colored *bigon* (it is an even polygon, where the edges are alternatively colored  $i$  and  $j$ ). Denote by  $b(\mathcal{H})$  the total number of  $ij$ -gons for  $0 \leq i < j \leq 3$ . Denote by  $t(\mathcal{H})$  the total number of  $\bar{i}$ -residues for  $0 \leq i \leq 3$ , where  $\bar{i}$  means complement of  $\{i\}$  in  $\{0, 1, 2, 3\}$ .

We briefly recall the definition of gems taken from [4]. A 3-gem is a  $(3 + 1)$ -graph  $\mathcal{H}$  satisfying  $v(\mathcal{H}) + t(\mathcal{H}) = b(\mathcal{H})$ . This relation is equivalent to having the vertices, edges and bigons restricted to any  $\{i, j, k\}$ -residue inducing a plane graph where the faces are bounded by the bigons. Therefore we can embed each such  $\{i, j, k\}$ -residue into a sphere  $\mathbb{S}^2$ . We consider the ball bounded this  $\mathbb{S}^2$  as induced by the  $\{i, j, k\}$ -residue. For this reason an  $\{i, j, k\}$ -residue in a 3-gem,  $i < j < k$ , is also called a *triball*. An  $ij$ -gon appears once in the boundary of triball  $\{i, j, k\}$  and once in the boundary of triball  $\{i, j, h\}$ . By pasting the triballs along disks bounded by all the pairs of  $ij$ -gons,  $\{i, j\} \subset \{0, 1, 2, 3\}$  of a gem  $\mathcal{H}$ , we obtain a closed 3-manifold denoted by  $|\mathcal{H}|$ . This general construction is dual to the one exemplified in the abstract and produces any closed 3-manifold. The manifold is orientable if and only if  $\mathcal{H}$  is bipartite, [8]. A *crystallization* is a gem which remains connected after deleting all the edges of any given color, that is, it has one  $\{i, j, k\}$ -residue for each trio of colors  $\{i, j, k\} \subset \{0, 1, 2, 3\}$ .

Let  $\mathcal{H}^*$  be the dual of a gem  $\mathcal{H}$ . An  $\bar{i}$ -residue of  $\mathcal{H}$  corresponds in  $\mathcal{H}^*$  to a 0-simplex of  $\mathcal{H}^*$ . Most 0-simplices of  $\mathcal{H}^*$  do not correspond to  $\bar{i}$ -residues of  $\mathcal{H}$ . An  $ij$ -gon of a gem  $\mathcal{H}$  corresponds in  $\mathcal{H}^*$  to a *PL1-face* formed by a sequence of 1-simplices of  $\mathcal{H}^*$ ; this PL1-face is the intersection of two PL2-faces of colors  $i$  and  $j$ ; their two bounding 0-simplices correspond to an  $\bar{h}$ - and to a  $\bar{k}$ -residue, where  $\{h, i, j, k\} = \{0, 1, 2, 3\}$ . An  $i$ -colored edge of  $\mathcal{H}$  corresponds to a *PL2-face* which is a 2-disk triangulated by a subset of  $i$ -colored 2-simplices of  $\mathcal{H}^*$ . Finally to a vertex of  $\mathcal{H}$ , it corresponds a *PL3-face* of  $\mathcal{H}^*$  which is a 3-ball formed by a subset of 3-simplices of  $\mathcal{H}^*$ .

**(1.1) Proposition.** *The 3-manifold induced by a  $J^2$ -gem  $\mathcal{H}$  is  $\mathbb{S}^3$ .*

**Proof.** Removing from  $\mathcal{H}$  all the edges of a given color still yields a connected graph which a plane graph and they come embedded so that the faces are the 2-residues. So  $\mathcal{H}$  has four 3-residues, one of each type. Denote by  $b_{ij}$  the number of  $ij$ -gons of  $\mathcal{H}$ . Each one of these residues are planar graphs having  $v = 2n$  vertices,  $3v/2$  edges and  $b_{12} + b_{13} + b_{23}$ ,  $b_{02} + b_{03} + b_{23}$ ,  $b_{01} + b_{13} + b_{03}$  and  $b_{12} + b_{01} + b_{02}$  faces for, respectively, the  $\bar{0}$ -,  $\bar{1}$ -,  $\bar{2}$ -,  $\bar{3}$ -residue. Adding the four formulas for the Euler characteristic of the sphere imply that  $v(\mathcal{H}) + 4 = b(\mathcal{H})$ . Therefore,  $\mathcal{H}$  is a crystallization having one  $0i$ -gon and one  $jk$ -gon. This implies that the fundamental group of the induced manifold is trivial: as proved in [3], the fundamental group of the space induced by a crystallization is generated by  $b_{0i} - 1$  generators, and in our case this number is 0. Since Poincaré Conjecture is now proved, we are done. However, we can avoid using this fact and, as a bonus, obtaining the validity of the next corollary, which is used in the sequel.

Assume that  $\mathcal{H}$  is a  $J^2$ -gem which does not induce  $\mathbb{S}^3$  and has the smallest possible number of vertices satisfying these assumptions. By planarity we must have a pair of edges of  $\mathcal{H}$  having the same ends  $\{p, q\}$ . Consider the graph  $\mathcal{H}fus\{p, q\}$  obtained from  $\mathcal{H}$  by removing the vertices  $p, q$  and the 2 edges linking them as well as welding the 2 pairs of pendant edges along edges of the same color. In [2] S. Lins proves that if  $\mathcal{H}$  is a gem,  $\mathcal{H}' = \mathcal{H}fus\{p, q\}$  is also a gem

and that two exclusive relations hold regarding  $|\mathcal{H}|$  and  $|\mathcal{H}'|$ , their induced 3-manifolds: either  $|\mathcal{H}| = |\mathcal{H}'|$  in the case that  $\{p, q\}$  induces a 2-dipole or else  $|\mathcal{H}| = |\mathcal{H}'| \# (\mathbb{S}^2 \times \mathbb{S}^1)$ . Since  $\mathcal{H}'$  is a  $J^2$ -gem, by our minimality hypothesis on  $\mathcal{H}$  the valid alternative is the second. But this is a contradiction: the fundamental group of  $|\mathcal{H}|$  would not be trivial, because of the summand  $\mathbb{S}^2 \times \mathbb{S}^1$ .  $\square$

### 1.3 Dipoles, pillows and balloons

Suppose there are  $m$  edges linking vertices  $x$  and  $y$  of a gem,  $m \in \{1, 2, 3\}$ . We say that  $\{u, v\}$  is an  $m$ -dipole if removing all edges in the colors of the ones linking  $x$  to  $y$ , these vertices are in distinct components of the graph induced by the edges in the complementary set of colors. To *cancel the dipole* means deleting the subgraph induced by  $\{u, v\}$  and identify pairs of the hanging edges along the same remaining color. To *create the dipole* is the inverse operation. It is simple to prove that the manifold of a gem is invariant under dipole cancellation or creation. Even though is not relevant for the present work state the foundational result on gems: two 3-manifolds are homeomorphic if and only if any two gems inducing it are linked by a finite number of cancellations and creations of dipoles, [1, 9].

The dual of a 2-dipole  $\{u, v\}$ , with internal colors  $i, j$  is named a *pillow*. It consists of two PL3-faces  $\nabla_u$  and  $\nabla_v$  sharing two PL2-faces colored  $i$  and  $j$ . The *thickening of a 2-dipole into a 3-dipole* is defined as follows. Let  $i, j$  be the two colors internal to 2-dipole  $\{u, v\}$  and  $k$  a third color. Let  $a$  be the  $k$ -neighbor of  $x$  and  $b$  be the  $k$ -neighbor of  $y$ . Remove edges  $[a, x]$  and  $[b, y]$  and put back  $k$ -edges  $[u, v]$  and  $[r, s]$ . This completes the thickening. It is simple to prove that the thickening in a gem produces a gem. We must be carefull because the inverse blind inverse operation *thinning a 3-dipole* not always produces a gem. The catch is that the result of the thinning perhaps is not a 2-dipole. In this sense the thinning move is not local: we must make sure that the result is a 2-dipole. To the data needed in thinning a 3-dipole  $\{u, v\}$  with internal colors  $\{i, j, k\}$  we must add the  $k$ -edge  $[r, s]$ . Note that the  $k$ -edges  $[u, v]$  and  $[r, s]$  are in the same  $hk$ -gon, where  $h$  is the fourth color. Denote by  $\Delta_{rs}$  the dual of  $[r, s]$ . Let  $\nabla_u \cup \nabla_v \cup \Delta_{rs}$  be called a *balloon*. Note that it consists of 2 PL3-faces  $\nabla_u$  and  $\nabla_v$  sharing three PL2-faces in colors  $\{i, j, k\}$  together with a  $k$ -colored PL2-face whose intersection with  $\nabla_u \cup \nabla_v$  is a PL1-face corresponding to the dual of the  $hk$ -gon, where  $h$  is the fourth color. Let  $\nabla_u \cup \nabla_v$  be the *balloon's head* and let  $\Delta_{rs}$  be the *balloon's tail*.

### 1.4 The Strategy for obtaining the PL-embedding of the dual of a $J^2$ -gem

We want to find a PL-embedding for the dual,  $\mathcal{H}^*$ , of a  $J^2$ -gem  $\mathcal{H}$  into  $\mathbb{S}^3$ . To this end we remove one PL3-face of  $\mathcal{H}^*$  find in  $\mathbb{R}^3$  a PL-embedding of the complementary ball so that their union form PL-triangulated tetrahedron. After we use the inverse of a stereographic projection with center in the exterior of the triangulated tetrahedron. In this way we recover in  $\mathbb{S}^3$  the missing PL3-face.

In this work we describe the PL-embedded PL3-faces of  $\mathcal{H}^*$  into  $\mathbb{R}^3$  by making it geometrically clear that its boundary is a set of 4 PL2-faces, one of each color, forming an embedded  $\mathbb{S}^2$  whose interior is disjoint from the interior of  $\mathbb{S}^2$ 's corresponding to others PL3-faces. Thus, for our purposes it will be only necessary to embed the 2-skeleton of  $\mathcal{H}^*$ .

A direct approach to find the PL-embedding of the dual of a general  $J^2$ -gem with  $2n$  vertices, seems very hard. Therefore, we split the algorithm into 4 phases.

In the first phase we find a sequence of  $n - 1$  2-dipole thickenings into 3-dipoles not using color 3, where the new involved edge is either 0 or 1 so that the final gem is simply a circular arrangement of  $n$  3-dipoles with internal colors 0, 1, 2. Such a canonical  $n$ -gem is named a *bloboid* and is denoted  $\mathcal{B}_n$ . Such 3-dipoles are also named a *blob over a 3-colored edge*. A  $J^2B$ -gem is a gem that, after cancelling blobs over 3-colored edge becomes a  $J^2$ -gem. This indexing decreasing sequence is easily obtainable from the primal objects, in the case, simplifying  $J^2B$ -gems until the bloboid is obtained:

$$\mathcal{H} = \mathcal{H}_n \xrightarrow[\text{thick}_1]{2\text{dip}} \mathcal{H}_{n-1} \xrightarrow[\text{thick}_2]{2\text{dip}} \dots \xrightarrow[\text{thick}_{n-1}]{2\text{dip}} \mathcal{H}_1 = \mathcal{B}_n = \mathcal{B}.$$

In the second phase we first find (phase 2A) specific abstract PL-triangulations, for the PL2-faces for the index increasing sequence of abstract colored 2-dimensional PL-complexes. Each of these complexes, latter, are going to be PL-embedded into  $\mathbb{R}^3$  so that the PL2-faces are topologically 2-spheres with disjoint interior. Attaching 3-balls bounded by these spheres we get the dual of the  $J^2$ -gem  $\mathcal{H}$  (with a vertex removed).

$$\mathcal{B}^* = \mathcal{H}_1^* \xrightarrow[\text{move}_1]{bp} \mathcal{H}_2^* \xrightarrow[\text{move}_2]{bp} \dots \xrightarrow[\text{move}_{n-1}]{bp} \mathcal{H}_n^* = \mathcal{H}^*.$$

In parallel to the construction of the sequence  $\mathcal{H}_m^*$ 's we also construct (phase 2B) a sequence of *wings*  $\mathcal{W}_m^*$ 's and their *nervures*  $\mathcal{N}_m^*$ 's so that  $\mathcal{W}_m^* \cup \mathcal{N}_m^*$  is an easy to define adequate planar graph:

$$\mathcal{W}_1^* \cup \mathcal{N}_1^* \xrightarrow[\text{move}_1]{wbp} \mathcal{W}_2^* \cup \mathcal{N}_2^* \xrightarrow[\text{move}_2]{wbp} \dots \xrightarrow[\text{move}_{n-1}]{wbp} \mathcal{W}_n^* \cup \mathcal{N}_n^* = \mathcal{W}^* \cup \mathcal{N}^*.$$

Each wing  $\mathcal{W}_m^*$ 's corresponds to a section of the previous sequence  $\mathcal{H}_m^*$ 's by two adequated fixed semi-planes  $\Pi_\ell$  and  $\Pi_r$ . The construction of the planar graphs  $\mathcal{W}_m^* \cup \mathcal{N}_m^*$  is recursive. Initially  $\mathcal{W}_1^*$  is a pincel of lines and  $\mathcal{N}_1^*$  is  $\emptyset$ . Going from  $\mathcal{W}_{m-1}^* \cup \mathcal{N}_{m-1}^*$  to  $\mathcal{W}_m^* \cup \mathcal{N}_m^*$  is very simple: two new vertices and four new edges appear, so as to maintain planarity.

In the third phase we make the abstract final element  $\mathcal{W}^* \cup \mathcal{N}^*$  of the second phase *rectilinearly* (that is each edge is a straihgt line segment) PL-embedded. By a cone construction we obtain from the rectilinearly PL-embedded  $\mathcal{W}^* \cup \mathcal{N}^*$  a special PL-complex, named  $\mathcal{H}_1^\diamond$ . This complex does not correpond to a gem dual and it can be loosely explained as  $\mathcal{H}_1^*$  with all balloon's heads "opened".

The fourth phase, the *pillow filling phase* starts with  $\mathcal{H}_1^\diamond$  and the uses the abstract sequence  $\mathcal{H}_m^*$ 's to produce a pillow filling sequence

$$\mathcal{H}_1^\diamond \xrightarrow[\text{filling}_1]{pillow} \mathcal{H}_2^\diamond \xrightarrow[\text{filling}_2]{pillow} \dots \xrightarrow[\text{filling}_{n-1}]{pillow} \mathcal{H}_n^\diamond = \mathcal{H}^*.$$

In this phase everything is embedded into  $\mathbb{R}^3$  and the last element is the PL-embedding that we seek.

The whole procedure can be implemented as a formal algorithm that takes  $O(n^2)$ -space and  $O(n^2)$ -time complexity, where  $2n$  is the number of vertices of the original  $J^2$ -gem.

## 1.5 Acknowledgements

We thank the anonymous referees, which made us think and provide an  $O(n)$ -solution for finding the wing sequence, instead of an  $O(n^3)$ -solution based on a bare Tutte's barycetric methods.

## 2 Details of the whole construction

### 2.1 First phase: from a $J^2$ -gem $\mathcal{H}$ to a bloboid $\mathcal{B}$

A  $k$ -dipole  $\{u, v\}$  involves color  $i$  if there is an edge of color  $i$  linking  $u$  to  $v$ . A blob is over

**(2.1) Proposition.** *Starting with a  $H$ -gem  $\mathcal{H}$  with  $2n$  vertices we can arrive to an  $n$ -bloboid  $\mathcal{B}$  by means of  $n - 1$  operations which thickens a 2-dipole involving color 2 into a 3-dipole, where the new edge is of color 0 or color 1, producing a sequence of  $J^2B$ -gems each inducing  $\mathbb{S}^3$ ,*

$$(\mathcal{H} = \mathcal{H}_n, \mathcal{H}_{n-1}, \dots, \mathcal{H}_2, \mathcal{H}_1 = \mathcal{B}).$$

**Proof.** The proof is by induction. For  $\ell = n$  we have  $\mathcal{H}_n = \mathcal{H}$  and so it is a  $J^2B$ -gem, establishing the basis of the induction. Assume that  $\mathcal{H}_\ell$  is a  $J^2B$ -gem. For  $\ell > 1$ , let  $\mathcal{H}'_\ell$  denote  $\mathcal{H}_\ell$  after cancelling the blobs. Since  $\mathcal{H}'_\ell$  is a  $J^2$ -gem by the Jordan curve theorem there is a vertex with two 2-dipoles incident to it. One of these dipole involve color 2 and the other involves color 3. Take the one involving color 2, name it  $D$ . Put back the blobs over the edges of color 3. So,  $D$  is present in  $\mathcal{H}_\ell$ . The colors involved in  $D$  are 0 and 2 or 1 and 2. In the first case we use color 1 to thicken  $D$  and in the second we use color 0 for the same purpose. This defines the  $J^2B$ -gem  $\mathcal{H}_{\ell-1}$ , which establishes the inductive step. In face of Proposition 1.1 and from the fact that thickening dipoles on gems produce gems inducing the same manifold, every member of the sequence induces  $\mathbb{S}^3$ .  $\square$

### 2.2 Second phase: colored abstract complexes, their wings, nervures

The second phase starts with an easy task, namely to define the dual of the bloboid, named  $\mathcal{H}_1^*$ . We get this first term in an embedded form. The others  $\mathcal{H}_2^*, \dots, \mathcal{H}_n^*$ , are, at this stage, obtained by slight modifications of the antecessor, but only in an abstract compinatorial way. In doing so we get the minimum level of refinement in the PL2-faces required, so that latter, the levels are sufficient for a geometric PL-embedding in  $\mathbb{R}^3$  which we seek.

#### 2.2.1 Colored abstract PL-complexes: $\mathcal{H}_1^*, \dots, \mathcal{H}_n^*$

We define the combinatorial 2-dimensional PL complex  $\mathcal{H}_1^*$  as follows.

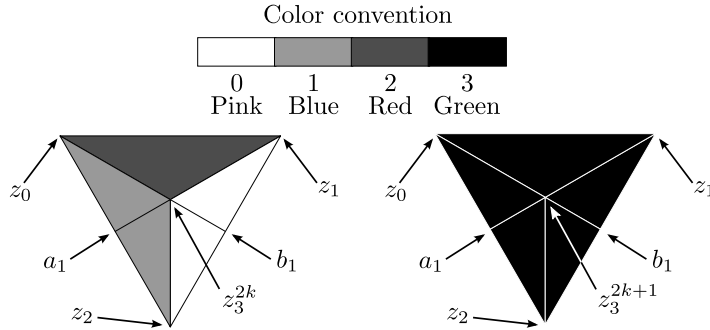


Figure 1: PL2-faces of  $\mathcal{H}_1^*$ .

The 0-simplices  $z_0, z_1$  and  $z_2$  are positioned in clockwise order as the vertices of an equilateral triangle of side 1 in the  $xy$ -plane so that  $z_0z_1$  is parallel to the  $x$ -axis and the center of the triangle coincides with the origin of an  $\mathbb{R}^3$ -cartesian system. The 0-simplex  $a_1$  is  $\frac{z_0+z_2}{2}$ . The 0-simplex  $b_1$  is  $\frac{z_2+z_1}{2}$ . Let the 0-simplices  $z_3^j$  be defined as  $z_3^j = (0, 0, 2n - j)$ ,  $1 \leq j \leq 2n$ , see Fig. 1.

We detail the connection with the  $J^2$ -gem. In particular we use the unique 23-gons of it to provide labels  $1, 2, \dots, 2n$  in the cyclic order of the 23-gon. This labellings correpond to PL3-faces of the  $\mathcal{H}_1^*$  and will be maintained for the PL3-faces of the whole remaining sequence  $\mathcal{H}_2^*, \dots, \mathcal{H}_n^*$ . This invariance is a dual manifestation of the fact that in the thickening of dipoles the labels of the vertices preserved. Suppose  $u$  is an odd vertex of the  $J^2$ -gem,  $u' = u - 1$ ,  $v = u + 1$  and  $v' = v + 1$ . The dual of a  $\bar{3}$ -residue is  $z_3^j$  where  $j$  is even. When  $j$  is odd, then  $z_3^j$  is a 0-simplex in the middle of a PL2<sub>3</sub>-face, incident to five 2-simplices of color 3. The dual of the 03-gon is the PL1-face formed by the pair of 1-simplices  $z_1b_1$  and  $b_1z_2$ . The dual of the 13-gon is the PL1-face formed by the pair of 1-simplices  $z_0a_1$  and  $a_1z_2$ . The dual of the 23-gon is the PL1-face formed by the 1-simplex  $z_0z_1$ . The dual of the 01-gon relative to vertices  $u$  and  $v$  is the 1-simplex  $z_2z_3^v$ . The dual of the 02-gon relative to vertices  $u$  and  $v$  is the 1-simplex  $z_1z_3^v$ . The dual of the 12-gon relative to vertices  $u$  and  $v$  is the 1-simplex  $z_0z_3^v$ . The dual of a 3-colored edge  $u'u$  is the image of PL2<sub>3</sub>-face with odd index  $u$  in the vertices. The dual of an  $i$ -colored edge  $uv$  with  $i \in \{0, 1, 2\}$  is the PL2 <sub>$i$</sub> -face with even index  $v$ .

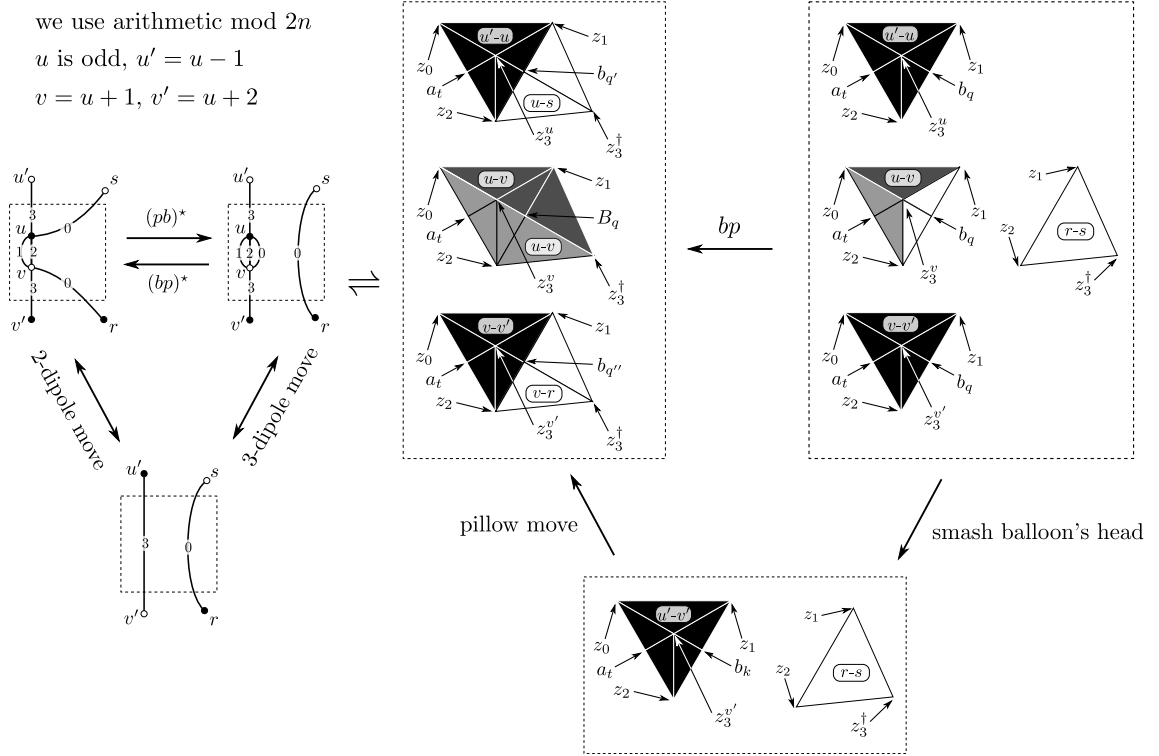


Figure 2: Primal and dual  $bp$ -moves.

Before presenting  $\mathcal{H}_m^*$ ,  $1 < m \leq n$ , and its embeddings, we need to understand the dual of the  $(pb)^*$ -move and its inverse. In the primal, to apply a  $(pb)^*$ -move, we need a blob and a 0- or 1-colored edge. The dual of this pair is the *balloon*: the *balloon's head* is the dual of the blob;

the *balloon's tail* is the dual of the  $i$ -edge. To make it easier to understand, the  $(pb)^*$ -move can be factorable into a 3-dipole move followed by a 2-dipole move, so in the dual, it is a smashing of the head of the balloon followed by the pillow move described in the book [4], page 39. This composite move is the *balloon-pillow move* or *bp-move*. Restricting our basic change in the colored 2-complex to *bp*-moves we have nice theoretical properties which are responsible for avoiding an exponential process. In what follows we describe the *bp*-move assuming that the balloon's tail is 0-colored using a generic balloon's tail, of which we just draw the contour, according to Fig. 2. The other case, color 1, is similar.

- i. if the image of  $v_5^u$  and  $v_5^v$  is  $b_q$ , create two 0-simplices  $b_{q'}$  and  $b_{q''}$ , define the images of  $v_5^u$  and  $v_5^{v'}$  as  $b_{q'}$  and  $b_{q''}$  and change the label of the image of  $v_5^v$  from  $b_q$  to  $B_q$ ;
- ii. make two copies of the PL2<sub>0</sub>-face, if necessary, refine each, from the middle vertex of the segment  $z_2 z_1$  to the third vertex  $z_3^\dagger$ , where  $\dagger = j$ , for an adequate height  $j$ ;
- iii. change the colors of the medial layer of the pillow as specified by the dual structure, namely by the current  $J^2 B$ -gem.

The choice of the letters  $P, B, R, G$  in the set *types* of next proposition comes from the colors  $0 = (P)ink$ ,  $1 = (B)lue$ ,  $2 = (R)ed$  and  $3 = (G)reen$ . In the next proposition,  $R_{2k-1}^b$  is a PL2<sub>2</sub>-face which is inside the pillow neighboring a PL2<sub>1</sub>-face. Similarly  $R_{2k-1}^p$  is a PL2<sub>2</sub>-face which is inside the pillow neighboring a PL2<sub>0</sub>-face.

**(2.2) Proposition.** *Each PL2-face of the combinatorial simplicial complex  $\mathcal{H}_m^*$ ,  $1 \leq m \leq n$ , is isomorphic to one in the set of types of triangulations*

$$\{G, P_{2k-1}, P'_{2k-1}, B_{2k-1}, B'_{2k-1}, R_{2k-1}^b, R_{2k-1}^p \mid k \in \mathbb{N}\},$$

*described in Fig. 3, where the index means the number of edges indicated and is called the rank of the type. Moreover, the PL2-faces that appear, as duals of the gem edges, have the minimum number of 2-simplices.*

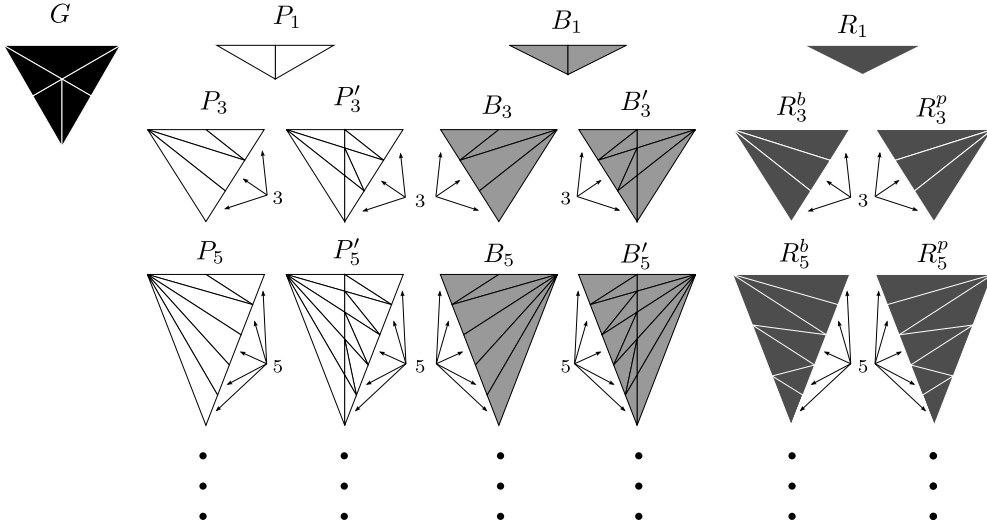


Figure 3: All kinds of PL2-faces that we use. These PL2-faces are for now abstract combinatorial triangulations that have the correct level of refinement so as to become PL-embedded into  $\mathbb{R}^3$

**Proof.** We need to fix a notation for the head of the balloon, instead of drawing all the PL2-faces of the head, we just draw one PL2<sub>3</sub>-face and put a label  $u'-v'$ . If the balloon's tail, is of type  $P_1$ , by applying a  $bp$ -move we can see at Fig. 4 that we get a PL2<sub>1</sub>-face of type  $B_3$

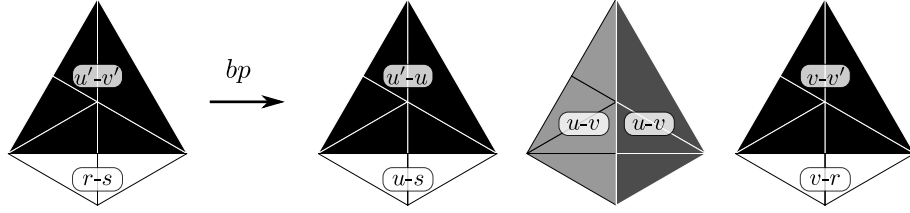


Figure 4:  $bp$  move with balloon's tail of type  $P_1$ .

and a PL2<sub>2</sub>-face of type  $R_3^b$ . The others PL2-faces are already known. If the balloon's tail, is of type  $B_3$ , by applying a  $bp$ -move, we need to refine the tail and the copies, otherwise we would not be able to build a pillow because some 2-simplices would be collapsed, so we get two PL2<sub>1</sub>-faces of type  $B'_3$ , one PL2<sub>0</sub>-face of type  $P_5$  and a PL2<sub>2</sub>-face  $R_5^p$ . The others PL2-faces are already known.

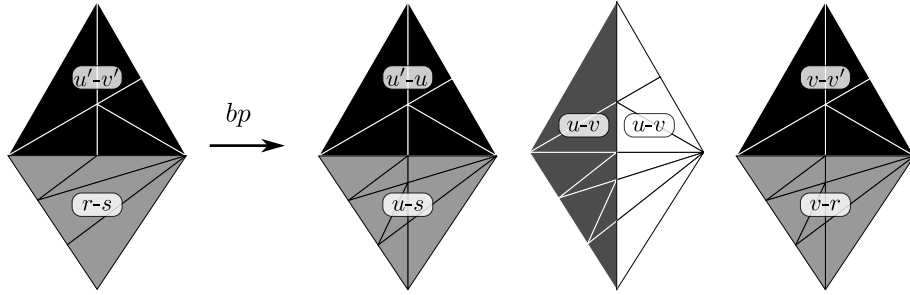


Figure 5:  $bp$  move with balloon's tail of type  $B_3$ .

In what follows given  $X \in \{P'_{2k-1}, B'_{2k-1}\}$  denote by  $\overline{X}$  the copy of  $X$  which is a PL2-face of the PL-tetrahedra whose PL2<sub>3</sub>-face is below the similar PL2<sub>3</sub>-face of the other PL-tetrahedra which completes the pillow in focus. In face of these conventions, if balloon's tail is of type

- $P_{2k-1}$ , then by applying a  $bp$ -move, we get types  $P'_{2k-1}, \widehat{P}'_{2k-1}, B_{2k+1}, R_{2k-1}^b$
- $P'_{2k-1}$ , then by applying a  $bp$ -move, we get types  $P_{2k-1}, B_{2k+1}, R_{2k-1}^b$
- $B_{2k-1}$ , then by applying a  $bp$ -move, we get types  $B'_{2k-1}, \widehat{B}'_{2k-1}, P_{2k+1}, R_{2k-1}^p$
- $B'_{2k-1}$ , then by applying a  $bp$ -move, we get types  $B_{2k-1}, P_{2k+1}, R_{2k-1}^p$

The necessary increasing in the ranks of the types of faces shows that the rank of each face is at least the one obtained. It may cause a surprise the fact that these ranks are enough to make the PL-embedding geometric into  $\mathbb{R}^3$ .  $\square$

It is worthwhile to mention, in view of the above proof, that each PL2-face is refined at most one time. So, if  $X$  is a type of PL2-face,  $X'$  is its refinement, then  $X'' = X'$ . This



idempotency is a crucial property inhibiting the exponentiality of our algorithm and enables a quadratic bound..

**(2.3) Corollary.** *The quadratic expressions*

$$3n^2 - 5n + 9, \quad 11n^2 - 17n + 21, \quad 8n^2 - 10n + 12$$

*are upper bounds for the numbers of 0-simplices, 1-simplices and 2-simplices of the colored 2-complex  $\mathcal{H}_n^*$  induced by a resolvable gem  $G$  with  $2n$  vertices.*

**Proof.**

We prove the first bound, on 0-simplices the other are similar: in the worse case, the increase of simplices is a linear function on the rank of the current PL2-face, and to get the final number we sum an arithmetic progreesion.

We detail the strategy for 0-simplexes. Note that  $\mathcal{H}_1^*$  has exactly  $z_0, z_1, z_2, a_1, b_1$  and  $z_3^j, j \in \{1, \dots, 2n\}$  as 0-simplices, which is  $2n + 5$  0-simplices. In the first step, the balloon's tail has to be of type  $P_1$  or  $B_1$ , so by applying a  $bp$ -move, we get two new 0-simplices. In second step, the worst case is when the balloon's tail is of type  $P_3$  or  $B_3$ , generated by last  $bp$ -move, so we add  $6 \times 1 + 2 = 8$  to the number of 0-simplices in the upper bound. In step  $k$  we note that the worst case is when we use the greatest ranked PL2-face generated by last  $bp$ -move, therefore the balloon's tail has to be of type  $P_{2k-1}$  or  $B_{2k-1}$  and we add  $6 \cdot (k - 1) + 2$  0-simplices. By adding the number of 0-simplices created by  $bp$ -moves from step 1 until step  $k$  we get  $3k^2 - k$  0-simplices. Since the number of steps is  $n - 1$ , and we have at the begining  $2n + 5$  0-simplices, we have that  $3n^2 - 5n + 9$  is an upper bound for the number of 0-simplices.  $\square$

### 2.2.2 Wings and their nervures: $\mathcal{H}_m \longleftrightarrow \mathcal{W}_m \cup \mathcal{N}_m, m = 1, \dots, n$

At some point in our research it became evident that what was needed to obtain the embedded PL-complex  $\mathcal{H}_n^*$  was a proper embedding into  $\mathbb{R}^3$  of two special sets of 0-simplices  $\{a'_1, a'_2, \dots, a'_f\}$  and  $\{b'_1, b'_2, \dots, b'_g\}$ , where  $f + g = 2n$ . Each  $a'_i \in \{a_i, A_i\}$  and each  $b'_i \in \{b_i, B_i\}$ . This terminology for the 0-simplices is obtained recursively and detailed at the proper location. For now we just say that all other 0-simplices are obtained by bisections of segments linking previously defined points. It came as a surprise to discover that this apparently difficult 3D problem can be reformulated as a plane problem with an easy solution, via a linear algorithm. That is the role of the wings and nervures corresponding to the colored complexes. The wing  $\mathcal{W}_m$  is a planar graph so that  $\mathcal{W}_m \setminus Z$  is a forest with two trees. The nervure of  $\mathcal{W}_m$ , denoted  $\mathcal{N}_m$  is a pair of trees which is the disjoint union of  $\mathcal{N}_m^\ell$  and  $\mathcal{N}_m^r$  with edge set disjoint from  $\mathcal{W}_m$  satisfying  $\mathcal{W}_m \cup \mathcal{N}_m \setminus \delta(Z) = \mathcal{N}_m$ .

Let  $\Pi_\ell$  ( $\Pi_r$ ) be the half plane limited by the  $z$ -axis which contains  $a_1 = z_0 z_2 / 2$  ( $b_1 = z_1 z_2 / 2$ ).

The construction of the wings and nervures of the next section are exemplified in Figs. 10 to 20.

We construct a sequence of pairs of plane graphs  $\{\{\mathcal{W}_1^\ell, \mathcal{W}_1^r\}, \{\mathcal{W}_2^\ell, \mathcal{W}_2^r\}, \dots, \{\mathcal{W}_n^\ell, \mathcal{W}_n^r\}\}$ . The  $m$ -th such pair constitutes the *left* and *right wings* of the colored 2-complex  $\mathcal{H}_m^*$ . The left wings are embedded into  $\Pi_\ell$  and the right wings are embedded into  $\Pi_r$ . We define  $\mathcal{W}_1^\ell$  as the set of  $2n$  straight line segments  $a_1 z_3^1, a_1 z_3^2, \dots, a_1 z_3^{2n} \subseteq \Pi_\ell$ , and  $\mathcal{W}_1^r$  as the set of  $2n$  straight line segments  $b_1 z_3^1, b_1 z_3^2, \dots, b_1 z_3^{2n} \subseteq \Pi_r$ . The *outer triangular region of the left wings* is the plane region spanned by  $a_1, z_3^1, z_3^{2n}$ . The *outer triangular region of the right wings* is the plane region spanned by  $b_1, z_3^1, z_3^{2n}$ . The passage from  $\{\mathcal{W}_{m-1}^\ell, \mathcal{W}_{m-1}^r\}$  to  $\{\mathcal{W}_m^\ell, \mathcal{W}_m^r\}$  in the  $(m-1)$ -th  $bp$ -move, which we call a *wbp-move*, corresponds in  $(\mathcal{H}_{m-1}, \mathcal{H}_m)$  to either a 0-flip that subdivides a 13-gon into two (case where the tail of the balloon is of color 0) or else to a 1-flip that subdivides a 03-gon into two (case where the tail of the balloon's is of color 1). At this point, we need to define a tree called the *nervure of a wing*. This is done inductively. The first ones,  $\mathcal{W}_1^\ell$  and  $\mathcal{W}_1^r$  have, respectively the degenerated trees formed by single points  $a_1$  and  $b_1$  as their nervures. In the unique wing that changes with the  $bp$ -move, a vertex  $x_\ell$  corresponding to either a 13-gon or else to a 03-gon (in a way to be made clear in the poof of Lemma 2.4). The intersection of the balloon's head and its tail in  $\mathcal{H}_m^*$  is a PL1-face formed by two simplices meeting at a point  $a_p$  (if the tail of the balloon is of color 1) or  $b_q$ , if it is of color 0. Along the process we define the following auxiliary functions, with arguments  $1 \leq m \leq n-1$ :  $c(m), u(m), v(m), r(m), s(m), \ell_a(m), \ell_b(m), t_a(m), t_b(m)$ . The color of the  $m$ -th balloon's tail is denoted by  $c(m) \in \{0, 1\}$ . Let  $u(m), v(m)$  be the odd and even indices of the  $m$ -th balloon's head  $\nabla_{u(m)} \cup \nabla_{v(m)}$ . Let  $r(m), s(m)$  be the odd and even indices of the  $m$ -th balloon's tail given by the  $\text{PL2}_{c(m)}$ -face  $\subseteq \nabla_{r(m)} \cap \nabla_{s(m)}$ . The positive integers  $\ell_a(m)$  and  $\ell_b(m)$  are the last  $a$ - and  $b$ -indices in left  $m$ -th wing and right  $m$ -th wing, respectively. Indices  $p$  or  $q$  in the  $m$ -th  $bp$ -move satisfy  $p = t_a(m)$  or  $q = t_b(m)$ . In the passage  $\mathcal{H}_m^*$  to  $\mathcal{H}_{m+1}^*$  either vertex  $a_p$  is replaced by  $a_{p'}, A_p, a_{p''}$ , where  $p' = \ell_a(m) + 1$  and  $p'' = \ell_a(m) + 2$  or else  $b_q$  is replaced by  $b_{q'}, B_p, b_{q''}$ , where  $q' = \ell_b(m) + 1$  and  $q'' = \ell_b(m) + 2$ , depending on the color of the balloon's tail. In the first case, we add two new edges  $a_{p'} A_p$  and  $a_{p''} A_p$  to the nervure, in the second case, we add the edges  $b_{q'} B_p$  and  $b_{q''} B_q$  to the nervure. In both cases,  $p'' = p' + 1$  or  $q'' = q' + 1$ . In the pictures the edges of the nervure are thicker than the ones in the respective wing. For  $1 \leq m \leq n$ , and  $h \in \{\ell, r\}$ , the nervure of  $\mathcal{W}_m^h$ , denoted  $\mathcal{N}_m^h$ , is a spanning tree of the graph  $\mathcal{W}_m^h \cup \mathcal{N}_m^h \setminus Z$ , where  $Z = \{z_3^j \mid j \in \{1, \dots, 2n\}\}$ . See Fig. 6, Fig. 7, Fig. 8 and the complete sequence of figures for the  $r_5^{24}$ -example, Figs. 10-20. A vertex in the tree  $\mathcal{N}_m^h$  is *pendant* if it has degree at most 1.

**(2.4) Lemma.** *Let  $1 \leq m \leq n$ . The set of pendant vertices of  $\mathcal{N}_m^\ell$  is in 1-1 correspondence with the set of 13-gons of  $\mathcal{H}_m$ . The set of pendant vertices in  $\mathcal{N}_m^r$  is in 1-1 correspondence with the 03-gons of  $\mathcal{H}_m$ .*

**Proof.** The intersection of the  $(m-1)$ -th balloon's head and tail is a PL1-face with two 1-simplices. Their intersection is a point in  $\Pi_h$ . The PL1-face dually corresponds to a 13-gon (resp. 03-gon) in  $\mathcal{H}_{m-1}$  if  $h = \ell$  ( $h = r$ ). After the 0-flip (resp. 1-flip) that produces  $\mathcal{H}_m$  the PL1-face is splitted into two, in a conformal way with the passage from  $\mathcal{W}_{m-1}^h \cup \mathcal{N}_{m-1}^h$  to  $\mathcal{W}_m^h \cup \mathcal{N}_m^h$ . Given this interpretation the Lemma is easily established by induction.  $\square$

A graph is *rectilinearly embedded into  $\mathbb{R}^3$*  if the images of their edges are straight line segments. We need to find by a linear algorithm a rectilinear embedding of the final pair of wings.

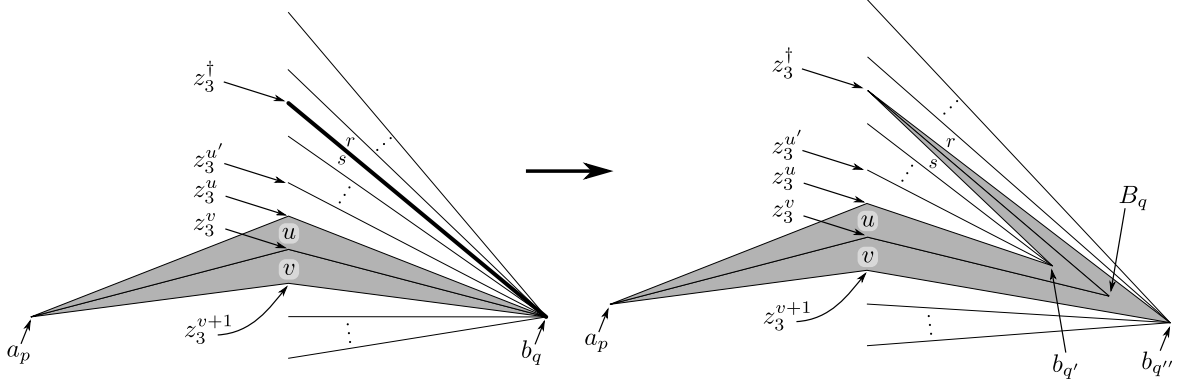


Figure 6: *wbp*-move: balloon's head section is painted in gray, and the part of balloon's tail that is intersecting the appropriate semi-plane is depicted as a *thick edge*.

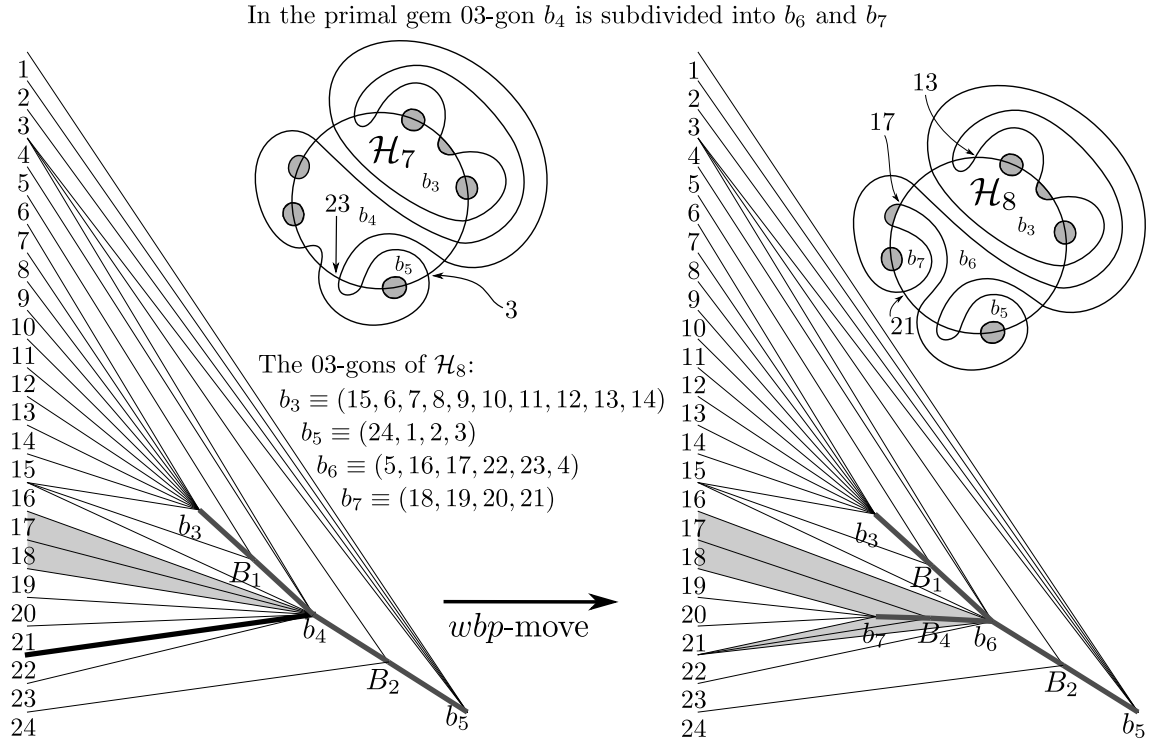


Figure 7: An example of *wbp*-move: four new edges and two new vertices are created. 0-simplex  $b_4$  corresponding to a 03-gon XXXXXXXXXXXXX

**(2.5) Lemma.** *The number of edges of  $\mathcal{W}_n^h \cup \mathcal{N}_n^h$ ,  $h \in \{\ell, r\}$  is at most  $6n - 4$ .*

**Proof.** The number of 1-simplices in the left wing and in the right wing of the initial complex in the sequence are both  $2n$ . At each one of the  $n - 1$  *bp*-moves we add 4 edges either to the left or to the right wing with its nervure. Thus each one of the final left and right wings with nervures has at most  $6n - 4$  edges.  $\square$

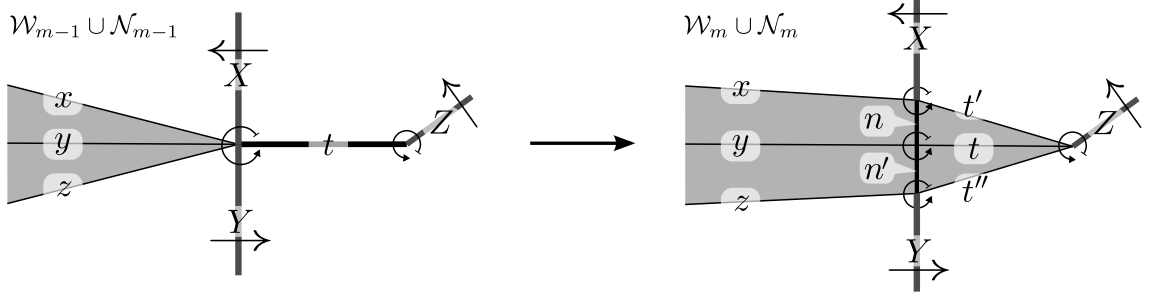


Figure 8: The general *wbp*-move: the *star* of a vertex of a graph embedded in an orientable surface (in our case the plane) is the counterclockwise cyclic sequence of edges incident to the vertex (such an ordering is induced by the surface). The set of stars is called a *rotation* and has the characterizing property that each edge appears twice. The general case of changing rotation when going from  $\mathcal{W}_{m-1} \cup \mathcal{N}_{m-1}$  to  $\mathcal{W}_m \cup \mathcal{N}_m$  is depicted above: the vertex  $XxyzYt$  breaks into three  $Xxnt'$ ,  $nyn't$  and  $n'zYt''$  and the vertex  $Zt$  changes into  $Zt'tt''$ . Two new vertices and four new edges are created. Two of these edges ( $n$  and  $n'$ ) are in the nervure  $\mathcal{N}_m$  and the other two ( $t'$  and  $t''$ ) are in the wing  $\mathcal{W}_m$ . The new rotation completely specifies the topological embedding of  $\mathcal{W}_m \cup \mathcal{N}_m$ .

### 2.3 Third phase: a rectilinear PL-embedding for $\mathcal{W}^* \cup \mathcal{N}^*$ and its induced $\mathcal{H}_1^\diamond$

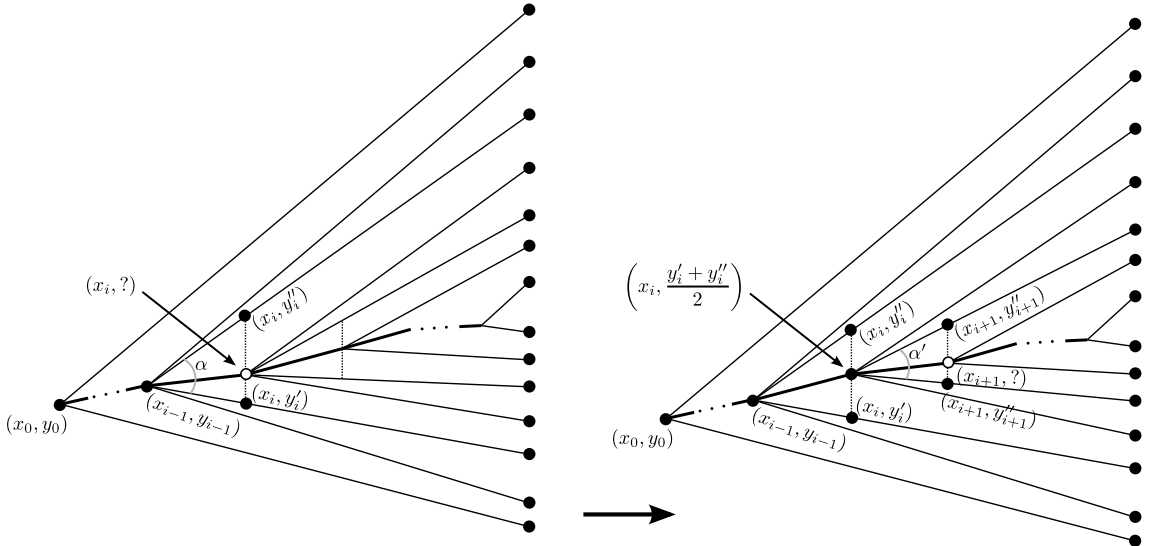


Figure 9: A linear algorithm for rectilinearly embedding one side of the last pair of wings (the other side is similar). In the general step we have the black vertices which are in their fixed position.

**2.4** Fourth phase: filling the pillows to obtain the PL-embedding of  $\mathcal{H}^*$  we seek

### **3 Conclusion and further work**

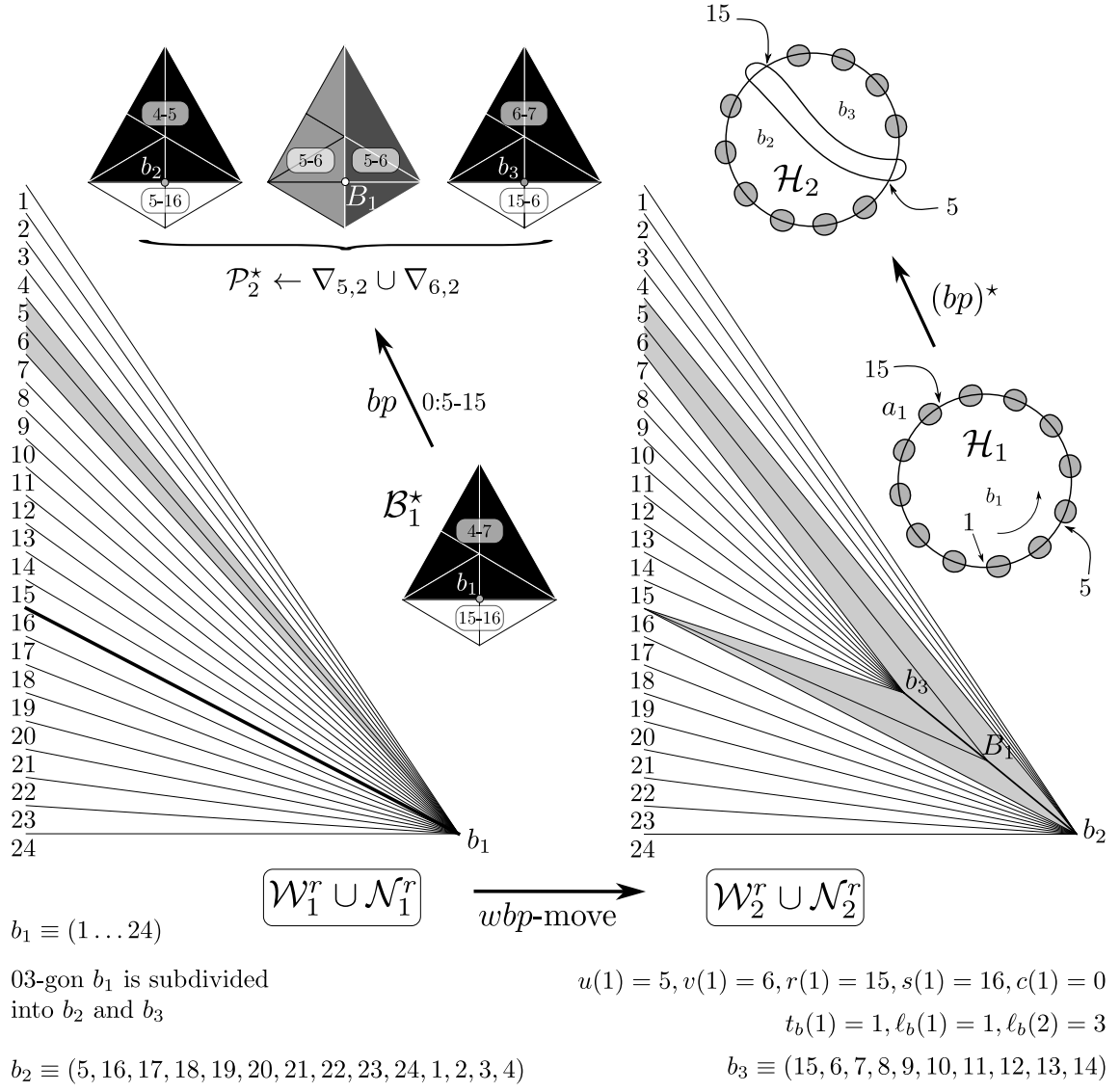
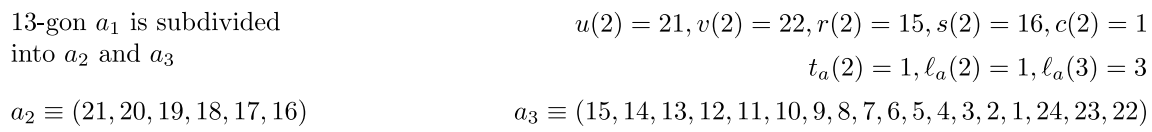
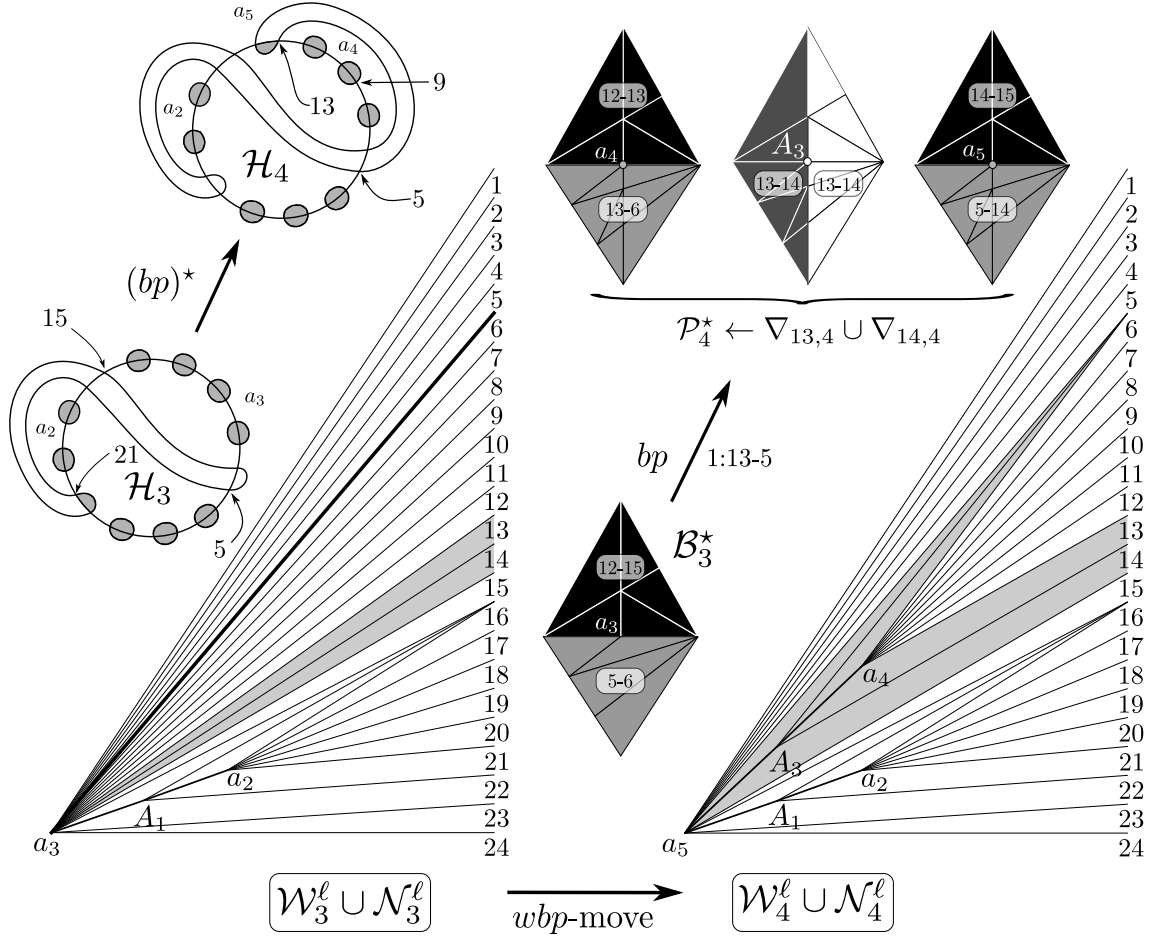


Figure 10:  $\mathcal{H}_2^* \leftarrow \mathcal{H}_1^* \cup (\mathcal{P}_2^* \setminus \mathcal{B}_1^*)$ . Pillow  $\mathcal{P}_2^* \leftarrow \nabla_{5,12} \cup \nabla_{6,12}$  ( $r_5^{24}$ -example).



15



13-gon  $a_3$  is subdivided  
into  $a_4$  and  $a_5$

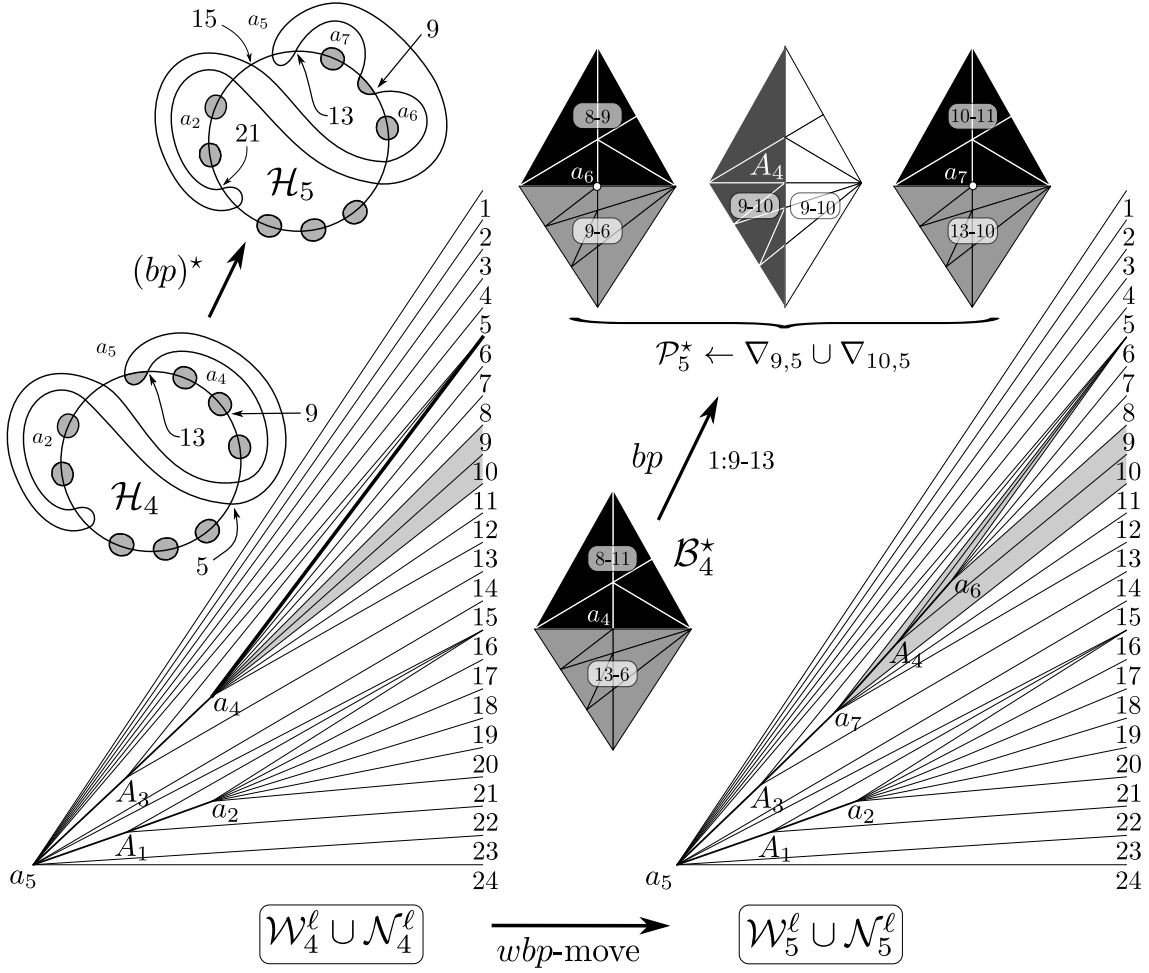
$$u(3) = 13, v(3) = 14, r(3) = 5, s(3) = 6, c(3) = 1$$

$$t_a(3) = 3, \ell_a(3) = 3, \ell_a(4) = 5$$

$$a_2 \equiv (21, 20, 19, 18, 17, 16) \quad a_4 \equiv (13, 12, 11, 10, 9, 8, 7, 6) \quad a_5 \equiv (15, 14, 5, 4, 3, 2, 1, 24, 23, 22)$$

Figure 12:  $\mathcal{H}_4^* \leftarrow \mathcal{H}_3^* \cup (\mathcal{P}_4^* \setminus \mathcal{B}_3^*)$ . Pillow  $\mathcal{P}_4^* \leftarrow \nabla_{13,12} \cup \nabla_{14,12}$  ( $r_5^{24}$ -example).





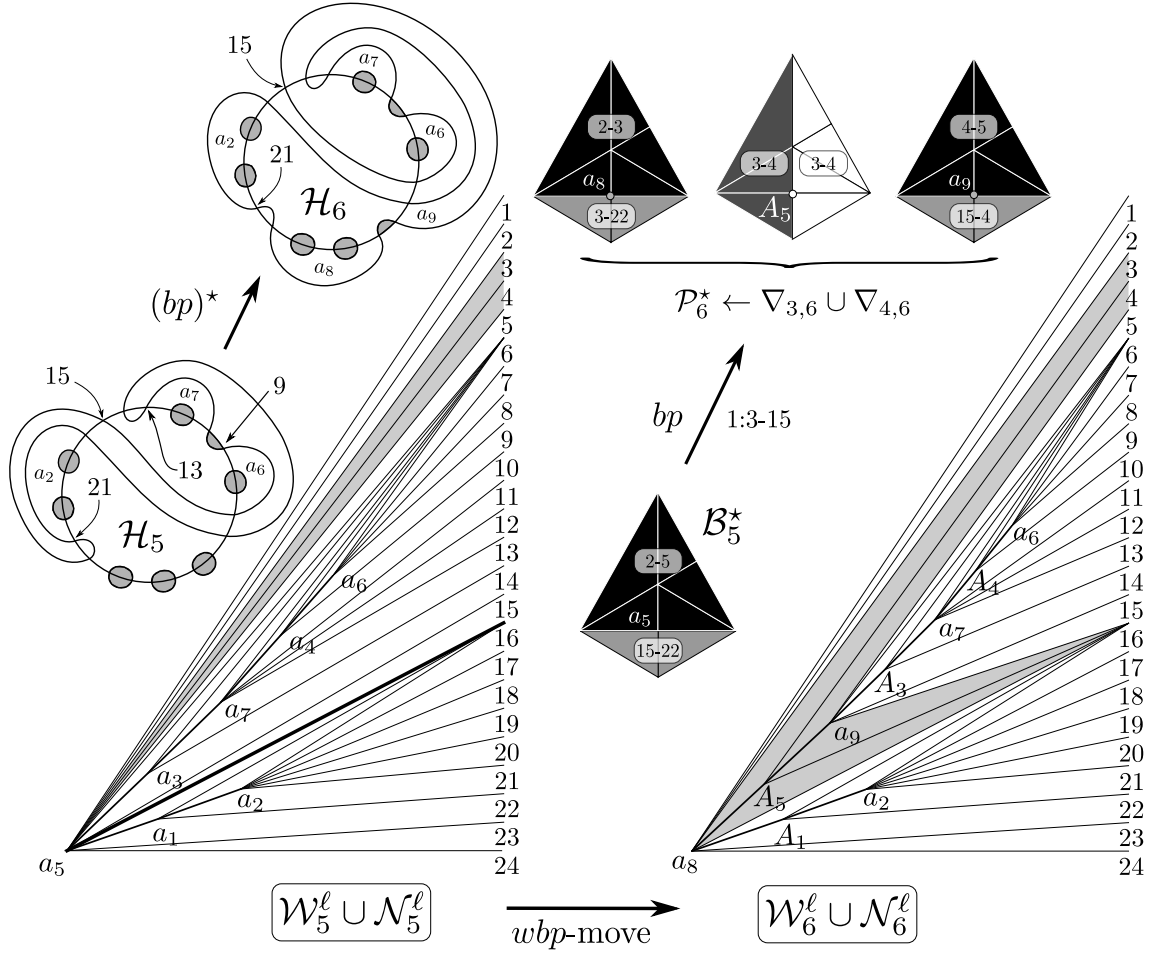
13-gon  $a_4$  is subdivided  
into  $a_6$  and  $a_7$

$$u(4) = 9, v(4) = 10, r(4) = 13, s(4) = 6, c(4) = 1$$

$$t_a(4) = 4, \ell_a(4) = 5, \ell_a(5) = 7$$

$$a_2 \equiv (21, 20, 19, 18, 17, 16) \quad a_5 \equiv (15, 14, 5, 4, 3, 2, 1, 24, 23, 22) \quad a_6 \equiv (9, 8, 7, 6) \quad a_7 \equiv (13, 12, 11, 10)$$

Figure 13:  $\mathcal{H}_5^\star \leftarrow \mathcal{H}_4^\star \cup (\mathcal{P}_5^\star \setminus \mathcal{B}_4^\star)$ . Pillow  $\mathcal{P}_5^\star \leftarrow \nabla_{9,12} \cup \nabla_{10,12}$  ( $r_5^{24}$ -example).



13-gon  $a_5$  is subdivided  
into  $a_8$  and  $a_9$

$$u(5) = 3, v(5) = 4, r(5) = 15, s(5) = 22, c(5) = 1$$

$$t_a(5) = 5, \ell_a(5) = 7, \ell_a(6) = 9$$

$$a_2 \equiv (21, 20, 19, 18, 17, 16)$$

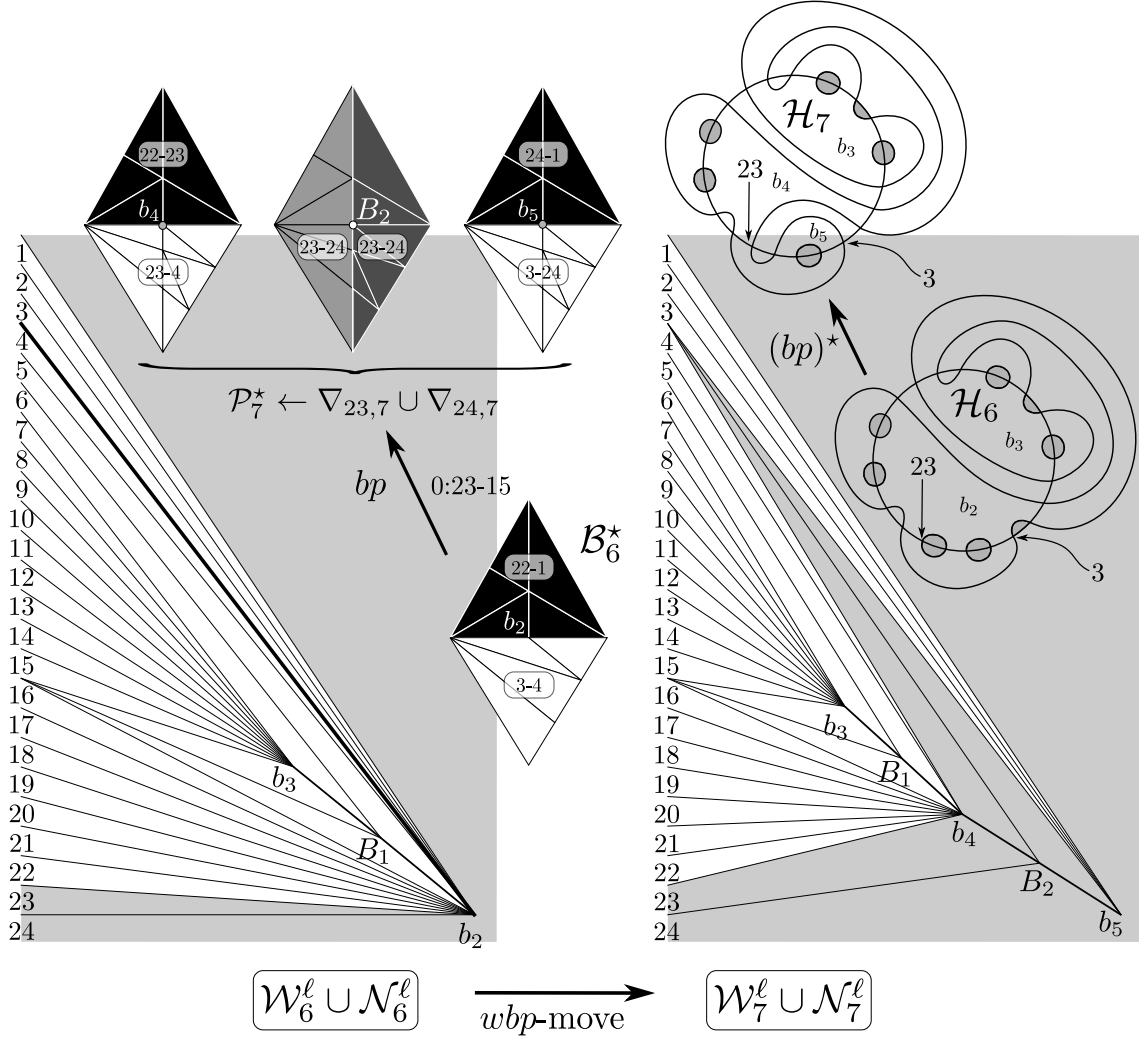
$$a_6 \equiv (9, 8, 7, 6)$$

$$a_7 \equiv (13, 12, 11, 10)$$

$$a_8 \equiv (3, 2, 1, 24, 23, 22)$$

$$a_9 \equiv (15, 14, 5, 4)$$

Figure 14:  $\mathcal{H}_6^* \leftarrow \mathcal{H}_5^* \cup (\mathcal{P}_6^* \setminus \mathcal{B}_5^*)$ . Pillow  $\mathcal{P}_6^* \leftarrow \nabla_{3,12} \cup \nabla_{4,12}$  ( $r_5^{24}$ -example).



03-gon  $b_2$  is subdivided  
into  $b_4$  and  $b_5$

$$u(6) = 23, v(6) = 24, r(6) = 3, s(6) = 4, c(6) = 0$$

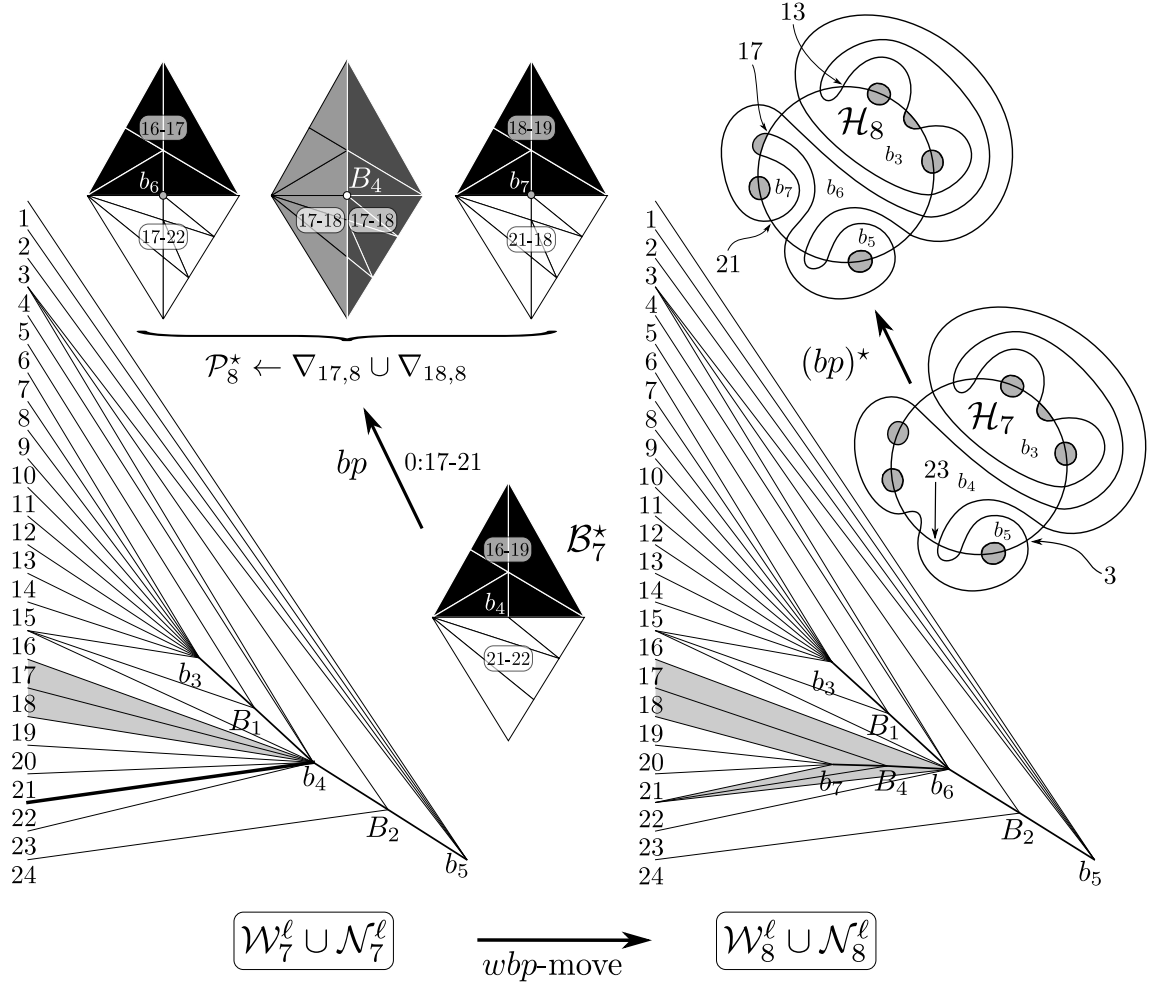
$$t_b(6) = 2, \ell_b(6) = 3, \ell_b(7) = 5$$

$$b_3 \equiv (15, 6, 7, 8, 9, 10, 11, 12, 13, 14)$$

$$b_4 \equiv (5, 16, 17, 18, 19, 20, 21, 22, 23, 4)$$

$$b_5 \equiv (24, 1, 2, 3)$$

Figure 15:  $\mathcal{H}_7^* \leftarrow \mathcal{H}_6^* \cup (\mathcal{P}_7^* \setminus \mathcal{B}_6^*)$ . Pillow  $\mathcal{P}_7^* \leftarrow \nabla_{23,12} \cup \nabla_{24,12}$  ( $r_5^{24}$ -example).



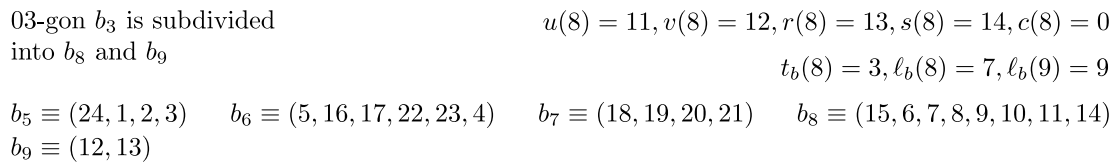
03-gon  $b_4$  is subdivided  
into  $b_6$  and  $b_7$

$$u(7) = 17, v(7) = 18, r(7) = 21, s(7) = 22, c(7) = 0$$

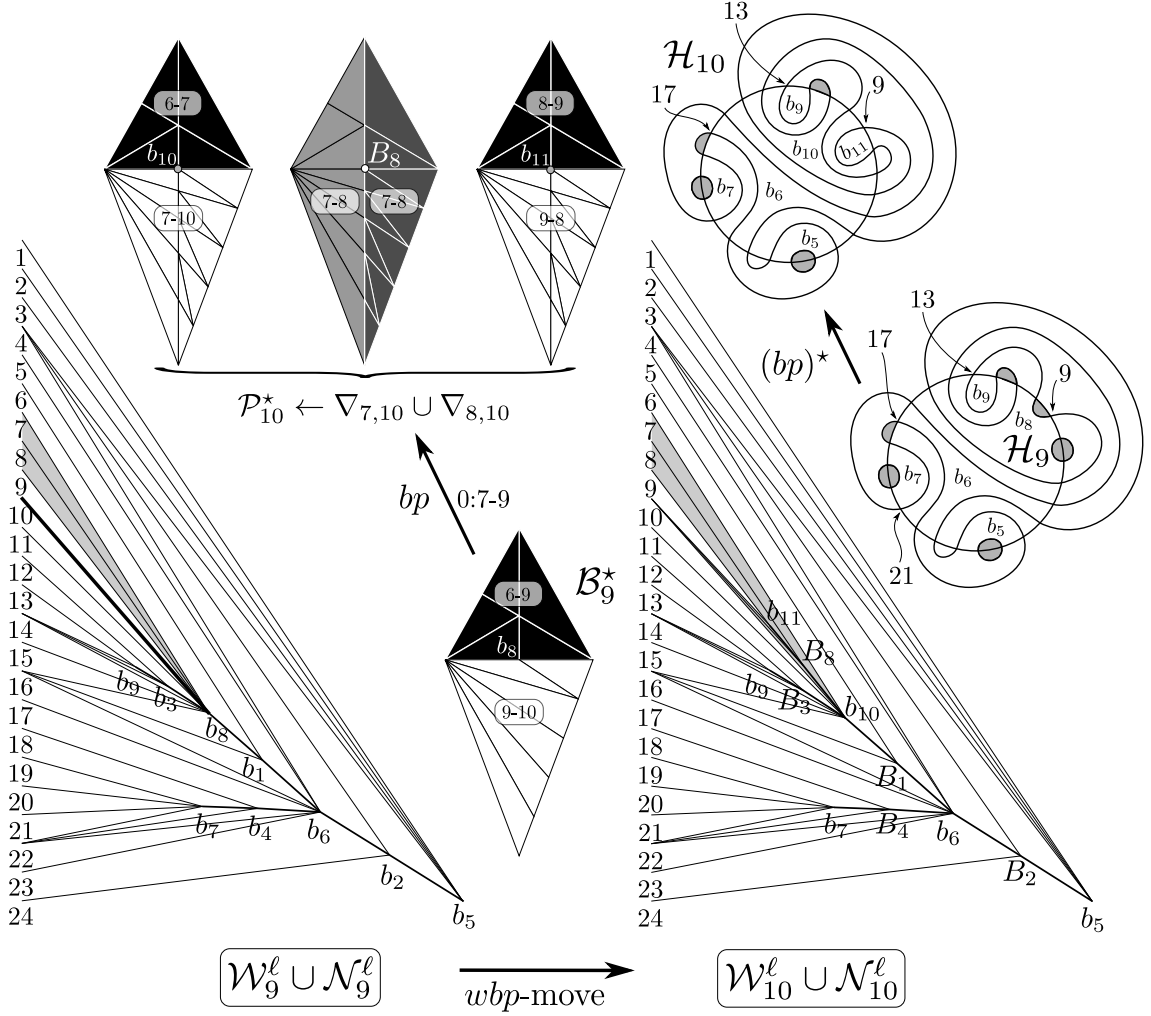
$$t_b(7) = 4, \ell_b(7) = 5, \ell_b(8) = 7$$

$$b_3 \equiv (15, 6, 7, 8, 9, 10, 11, 12, 13, 14) \quad b_5 \equiv (24, 1, 2, 3) \quad b_6 \equiv (5, 16, 17, 22, 23, 4) \quad b_7 \equiv (18, 19, 20, 21)$$

Figure 16:  $\mathcal{H}_8^* \leftarrow \mathcal{H}_7^* \cup (\mathcal{P}_8^* \setminus \mathcal{B}_7^*)$ . Pillow  $\mathcal{P}_8^* \leftarrow \nabla_{17,12} \cup \nabla_{18,12}$  ( $r_5^{24}$ -example).



21



03-gon  $b_8$  is subdivided  
into  $b_{10}$  and  $b_{11}$

$$u(9) = 7, v(9) = 8, r(9) = 9, s(9) = 10, c(9) = 0$$

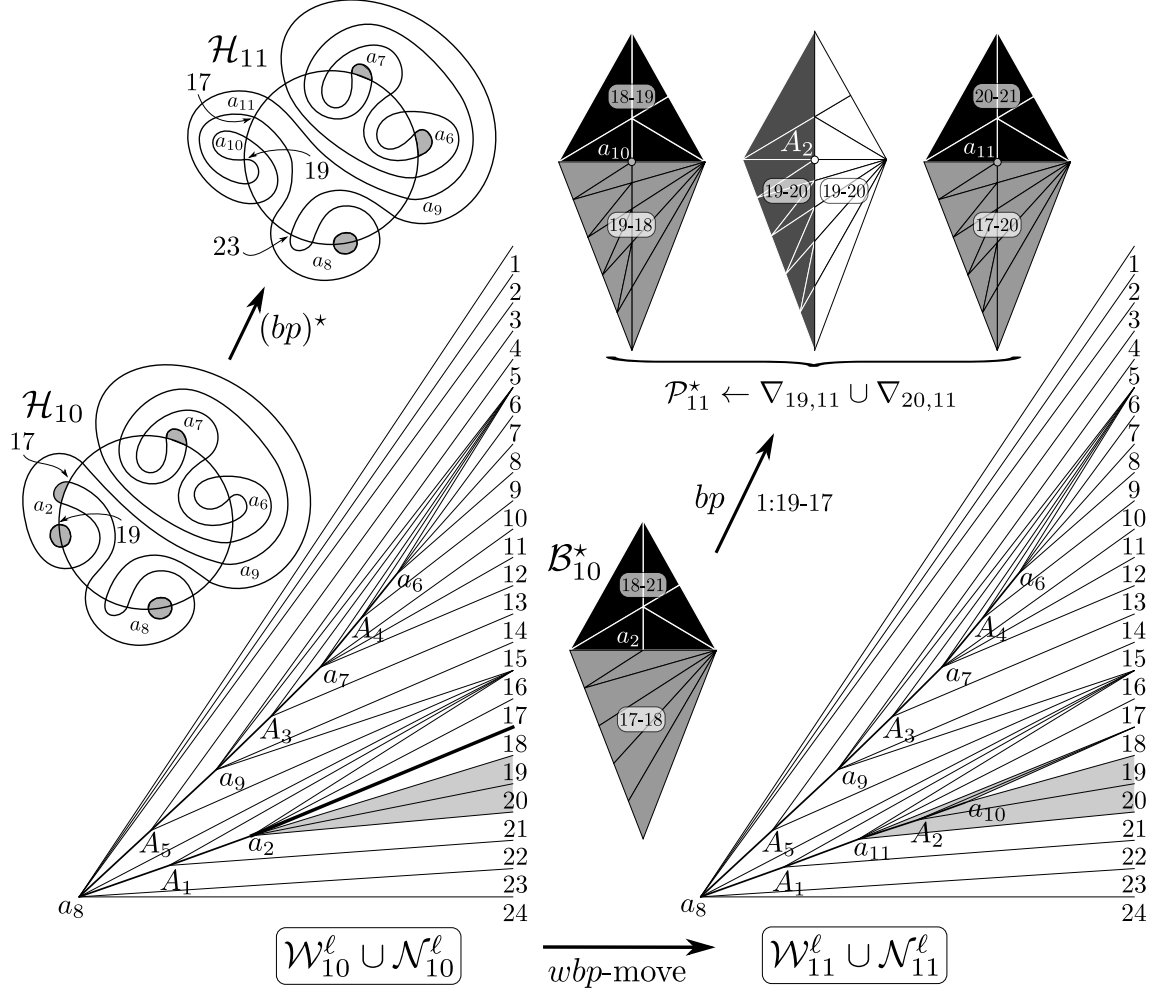
$$t_b(9) = 8, \ell_b(9) = 9, \ell_b(10) = 11$$

$$b_5 \equiv (24, 1, 2, 3) \quad b_6 \equiv (5, 16, 17, 22, 23, 4)$$

$$b_7 \equiv (18, 19, 20, 21) \quad b_9 \equiv (12, 13)$$

$$b_{10} \equiv (15, 6, 7, 10, 11, 14) \quad b_{11} \equiv (8, 9)$$

Figure 18:  $\mathcal{H}_{10}^* \leftarrow \mathcal{H}_9^* \cup (\mathcal{P}_{10}^* \setminus \mathcal{B}_9^*)$ . Pillow  $\mathcal{P}_{10}^* \leftarrow \nabla_{7,12} \cup \nabla_{8,12}$  ( $r_5^{24}$ -example).



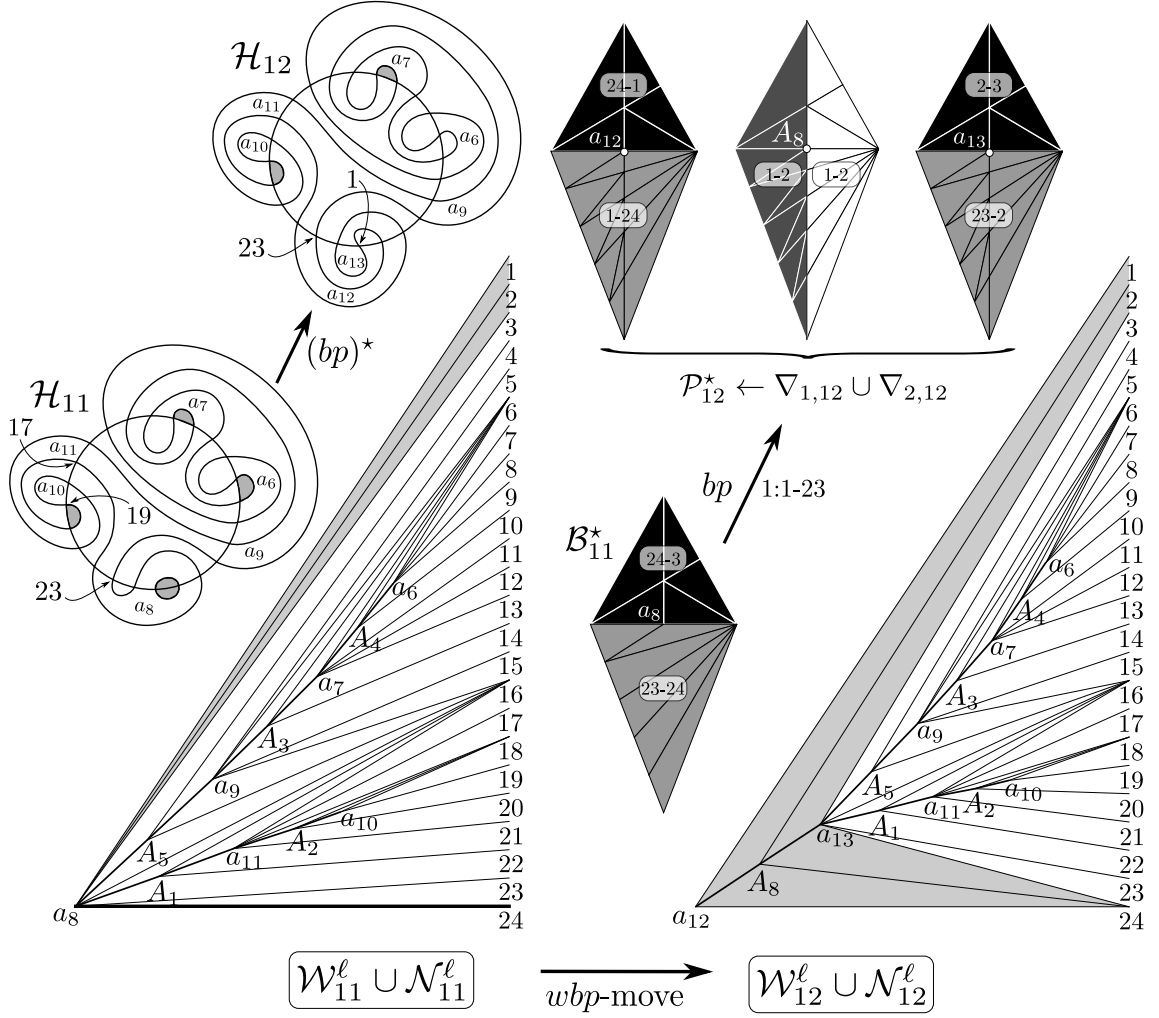
13-gon  $a_2$  is subdivided  
into  $a_{10}$  and  $a_{11}$

$$u(10) = 19, v(10) = 20, r(10) = 17, s(10) = 18, c(10) = 1$$

$$t_a(10) = 2, \ell_a(10) = 9, \ell_a(11) = 11$$

$$a_6 \equiv (9, 8, 7, 6) \quad a_7 \equiv (13, 12, 11, 10) \quad a_8 \equiv (3, 2, 1, 24, 23, 22) \quad a_9 \equiv (15, 14, 5, 4) \quad a_{10} \equiv (19, 18) \\ a_{11} \equiv (21, 20, 17, 16)$$

Figure 19:  $\mathcal{H}_{11}^* \leftarrow \mathcal{H}_{10}^* \cup (\mathcal{P}_{11}^* \setminus \mathcal{B}_{10}^*)$ . Pillow  $\mathcal{P}_{11}^* \leftarrow \nabla_{19,12} \cup \nabla_{20,12}$  ( $r_5^{24}$ -example).



13-gon  $a_8$  is subdivided  
into  $a_{12}$  and  $a_{13}$

$$u(11) = 1, v(11) = 2, r(11) = 23, s(11) = 24, c(11) = 1$$

$$t_a(11) = 8, \ell_a(11) = 1$$

$$a_6 \equiv (9, 8, 7, 6) \quad a_7 \equiv (13, 12, 11, 10) \quad a_9 \equiv (15, 14, 5, 4) \quad a_{10} \equiv (19, 18) \quad a_{11} \equiv (21, 20, 17, 16)$$

$$a_{12} \equiv (3, 2, 23, 22) \quad a_{13} \equiv (1, 24)$$

Figure 20:  $\mathcal{H}_{12}^* \leftarrow \mathcal{H}_{11}^* \cup (\mathcal{P}_{12}^* \setminus \mathcal{B}_{11}^*)$ . Pillow  $\mathcal{P}_{12}^* \leftarrow \nabla_{1,12} \cup \nabla_{2,12}$  ( $r_5^{24}$ -example).



## References

- [1] M. Ferri and C. Gagliardi. Crystallisation moves. *Pacific J. Math*, 100(1):85–103, 1982.
- [2] S. Lins. A simple proof of Gagliardi’s handle recognition theorem. *Discrete mathematics*, 57(3):253–260, 1985.
- [3] S. Lins. On the fundamental group of 3-gems and a planar class of 3-manifolds. *European Journal of Combinatorics*, 9(4):291–305, 1988.
- [4] S. Lins. *Gems, Computers, and Attractors for 3-Manifolds*. World Scientific, 1995.
- [5] S. Lins and R. Machado. Framed link presentations of 3-manifolds by an  $O(n^2)$  algorithm, I: gems and their duals. *arXiv:1211.1953v2 [math.GT]*, 2012.
- [6] S. Lins and R. Machado. Framed link presentations of 3-manifolds by an  $O(n^2)$  algorithm, II: colored complexes and boundings in their complexity. *arXiv:1212.0826v2 [math.GT]*, 2012.
- [7] S. Lins and R. Machado. Framed link presentations of 3-manifolds by an  $O(n^2)$  algorithm, III: geometric complex  $\mathcal{H}_n^*$  embedded into  $\mathbb{R}^3$ . *arXiv:1212.0827v2 [math.GT]*, 2012.
- [8] S. Lins and A. Mandel. Graph-encoded 3-manifolds. *Discrete Math.*, 57(3):261–284, 1985.
- [9] S. Lins and M. Mulazzani. Blobs and flips on gems. *Journal of Knot Theory and its Ramifications*, 15(8):1001–1035, 2006.
- [10] C.P. Rourke and B.J. Sanderson. *Introduction to piecewise-linear topology*, volume 69. Springer-Verlag, 1982.

Sóstenes L. Lins  
Centro de Informática, UFPE  
Av. Jornalista Aníbal Fernandes s/n  
Recife-PE 50740-560  
Brazil  
sostenes@cin.ufpe.br

Ricardo N. Machado  
Núcleo de Formação de Docentes, UFPE  
Av. Jornalista Aníbal Fernandes s/n  
Caruaru-PE  
Brazil  
ricardonmachado@gmail.com